



## EXPERIMENTAL ANALYSIS OF THE KINEMATICS IN THE ELASTIC COLLISION BETWEEN TWO BODIES DURING THE CONTACT TIME

### ANÁLISIS EXPERIMENTAL DE LA CINEMÁTICA EN LA COLISIÓN ELÁSTICA ENTRE DOS CUERPOS DURANTE EL TIEMPO DE CONTACTO

Suyana Arcos Villagómez<sup>1,\*</sup> , Santiago Álvaro Pillalaza<sup>2</sup> ,  
 Xavier Rivera Gálvez<sup>2</sup> , César Michelena Rosero<sup>2</sup> , Emilse Camacho Cañar<sup>2</sup> 

Received: 25-03-2024, Received after review: 21-05-2024, Accepted: 06-06-2024, Published: 01-07-2024

### Abstract

The elastic collision between two bodies is a fleeting event challenging to observe due to its infinitesimally short contact time, usually lasting mere hundredths or even thousandths of a second. This brief duration poses significant challenges for accurately measuring velocities and impulsive forces and establishing representative functions. Consequently, this study aims to address these challenges. Experimental measurements of velocity, acceleration, and force changes during the contact period are crucial for validating theoretical models and functions that accurately represent the dynamics of collisions under realistic conditions. These measurements are critical in optimizing the activation response of airbag and restraint systems in vehicles and are fundamental in reconstructing physical scenarios of accidents. The experiments were conducted in a practical computer-assisted laboratory, utilizing wireless sensors embedded within the test vehicles and positioned on a low-friction track. The collision setup was designed to be horizontal and frontal, ensuring that the bodies involved did not undergo permanent deformations. The primary methodology adopted in this analysis integrates both quantitative and qualitative approaches, focusing on collecting and analyzing numerical data to identify patterns and establish mathematical relationships between variables. This integrated approach offers a more comprehensive understanding of the kinematics of colliding vehicles during the contact period.

**Keywords:** elastic collision, two-body collision, contact time, two-body kinematics, coefficient of friction

### Resumen

La colisión elástica entre dos cuerpos es un evento rápido y difícil de observar, dado que el tiempo de contacto es infinitesimal, del orden de centésimas o incluso milésimas de segundo, por lo que surge el desafío de medir con precisión las velocidades y fuerzas impulsivas, así como establecer funciones representativas. En este trabajo se propone abordar precisamente ese objetivo. Las mediciones experimentales de la variación de la velocidad, aceleración y fuerza, durante el tiempo de contacto, desempeñan un papel esencial en la validación de modelos teóricos y funciones que describen el comportamiento de las colisiones en situaciones del mundo real. Estas mediciones permiten optimizar la respuesta de activación de los airbags, sistemas de retención en los automóviles, hasta reconstruir accidentes desde el punto de vista de la Física. La experimentación se llevó a cabo en un laboratorio práctico asistido por computadora, empleando sensores inalámbricos incorporados en los carros de prueba y dispuestos sobre una pista de bajo coeficiente de rozamiento. El escenario de la colisión fue horizontal y frontal, sin que los cuerpos sufrieran deformaciones permanentes. La metodología principal utilizada en este análisis es cuantitativa y cualitativa, enfocándose en la recopilación y estudio de datos numéricos para identificar patrones y relaciones matemáticas entre las variables. Este enfoque combinado permite una comprensión más completa de la cinemática de los carros en colisión durante el tiempo de contacto.

**Palabras clave:** choque elástico, colisión de dos cuerpos, tiempo de contacto, cinemática de dos cuerpos, coeficiente de rozamiento.

<sup>1,\*</sup>Escuela de Ingeniería de Sistemas, Facultad de Ingeniería, Pontificia Universidad Católica del Ecuador, Ecuador.  
 Corresponding author ✉: sfarcos@puce.edu.ec.

<sup>2</sup>Facultad de Ciencias Exactas y Naturales, Pontificia Universidad Católica del Ecuador, Ecuador.

Suggested citation: Arcos Villagómez, S.; Álvaro Pillalaza, S.; Rivera Gálvez, X.; Michelena Rosero, C. and Camacho Cañar, E. "Experimental analysis of the kinematics in the elastic collision between two bodies during the contact time," *Ingenius, Revista de Ciencia y Tecnología*, N.º 32, pp. 69-76, 2024, DOI: <https://doi.org/10.17163/ings.n32.2024.07>.

## 1. Introduction

In physics, conducting experiments is essential for understanding phenomena often assumed in theoretical contexts [1]. The study of frontal elastic collisions is particularly intriguing. In such collisions, the bodies involved do not undergo permanent deformations or exchange mass, fully separating after the impact [2]. The principles of conservation of kinetic energy and linear momentum are upheld both before and after the collision. Nonetheless, the dynamics occurring during the contact time between the colliding objects frequently remain underexplored.

Collisions between bodies are a fundamental focus within the field of physics, with the characterization of contact time during these collisions being particularly critical for this research. Contact time, the instantaneous interval during which the objects interact upon impact, is crucial in determining the forces exerted and the velocities of the colliding bodies. The inherent complexity of this phenomenon, especially in real-world settings, has substantially limited the ability to fully understand it.

Contact time during collisions can span mere hundredths or thousandths of a second, posing significant challenges for accurately collecting experimental data. The growing integration of technology in Physics laboratories enables the measurement of physical parameters over brief intervals, facilitating the documentation of rapid events that are imperceptible to the human observer and beyond the capabilities of traditional instruments [2]. In this context, the advancement of position and motion sensors is crucial. These technologies allow for the detailed capture of data on practically instantaneous processes during body collisions, providing valuable insights into their dynamics.

Contemporary physics laboratories are equipped with advanced data loggers, sophisticated digital devices that facilitate the connection of multiple sensors for comprehensive data collection. These tools play an integral role in conducting experiments, significantly enhancing the accuracy and efficiency of data acquisition.

Data loggers can be replaced by computers equipped with Bluetooth connectivity, enabling the receipt of sensor information. These sensors are transducers fitted with the technology to detect physical or chemical quantities, called instrumentation variables, and convert them into electrical signals [3].

In practical applications, physical quantities are inherently analog. To facilitate their processing and utilization in digital devices, an analog-to-digital converter (ADC) is employed. However, these quantities undergo a preliminary stage before digitization, known as sampling frequency. This characteristic dictates the number of samples collected per second. Properly adjusting the sampling frequency is crucial for effectively

capturing the analog information, thereby minimizing data loss and enhancing conversion accuracy during digitization.

Sampling, also known as signal discretization, represents the initial step in converting an analog signal, characterized by continuous time and amplitude, into a digital signal, which features discrete time and amplitude. This process is fundamental to the accurate digital representation of analog data [4].

From this perspective, implementing sensor-equipped vehicles is proposed as an innovative approach to recreate elastic collisions and meticulously examine the events transpiring during the contact time between bodies.

In real-world applications, sensors are crucial for activating passive safety systems in vehicles. During an impact, the seatbelt pre-tensioner and airbag are passive safety systems. Key components of the airbag system include the control unit, the safing safety sensor, and the impact sensor. The safing safety sensor, integral to the airbag module, is connected to the frontal impact sensors. The impact sensor is designed to respond to a combination of force, acceleration, and duration [5]. Specifically, the acceleration sensor monitors changes in the vehicle's speed, while the impact sensor detects the force of frontal impacts, contributing to timely and effective safety responses [6].

An electronic control unit activates the airbag system, which operates based on signals received from the system's sensor. This sensor is strategically positioned to detect sudden decelerations resulting from a collision.

The airbag deploys in response to a sudden change in the vehicle's overall inertia, typically triggered by a frontal impact with an obstacle or another vehicle [7].

Simulating a frontal impact for biomechanical assessment using finite elements elucidates the advantages of incorporating airbags as passive safety elements [8]. This approach enhances the quality of this research and facilitates the exploration and validation of theoretical models within a practical and dynamic context.

The emerging challenge for Physics laboratories involves effectively utilizing the extensive information generated by sensors for detailed interpretation and analysis [9]. Meticulous and comprehensive analysis of this data is crucial for elucidating the underlying physical phenomena, validating existing theories, or generating new hypotheses. Such experimental data offer a solid empirical foundation that underpins scientific conclusions and enables researchers to make well-informed decisions regarding advancing theories and models.

## 2. Materials and Methods

Figure 1 summarizes the research methodology and illustrates the most relevant stages of the experimentation.

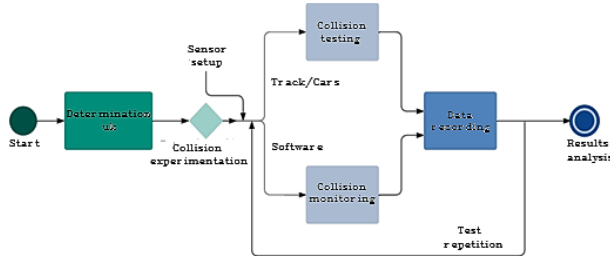


**Figure 1.** Diagram of the methodology used in the experimentation

To conduct the experimentation, the dynamic friction coefficient  $u_k$  between the thin plastic wheels of the cars and the aluminum track was determined. This was accomplished by positioning a car on the horizontal track and progressively increasing the inclination angle ( $\theta$ ) until the car began to move freely, reaching what is referred to as the kinetic friction angle ( $\theta_k$ ), [10].

The forces depicted in the free-body diagram [11] and the inclination angle were analyzed to derive the equation for determining the dynamic friction coefficient.

The mathematical formula used to calculate this coefficient is  $u_k = \tan(\theta_k)$  [12], as sourced from Serway's Physics book. This approach yielded an experimental dynamic friction coefficient of  $u_k = 0,009$ .

Subsequently, test vehicles equipped with wireless sensors, maintained in optimal conditions and with nearly identical masses, were utilized. The masses were approximately ( $m_1 = 0,5048kg$ ) and ( $m_2 = 0,5022kg$ ), respectively.

The vehicles were positioned frontally on the aluminum track, spaced one meter apart. A connection was established between the computer's Bluetooth system and the sensors to facilitate data collection.

The track was meticulously installed to ensure it was level and free from obstructions, thereby minimizing the loss of kinetic energy, as illustrated in Figure 2.

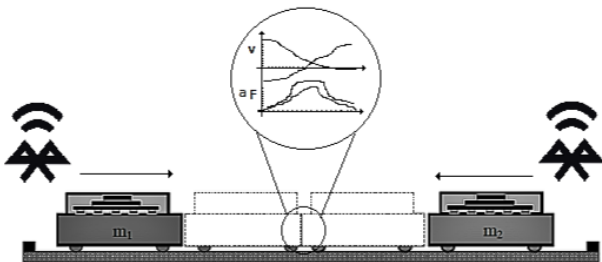


**Figure 2.** Schematic representation of the events occurring during the collision time

Similar springs exerting equivalent forces were used to initiate the cars' motion. These springs were integrated into the rear of each vehicle to provide the initial impulse. Upon release of the springs, the cars propelled in opposite directions, culminating in a collision.

The experiments confirmed that the contact time was 0.025 seconds, indicative of a rapid and potentially violent collision. During this brief interval, both the initial and final velocities were determined, representing the average values of the experimental data, as detailed in Table 1

**Table 1.** Car velocities during contact time

Time [s]	Car Velocity (1) [m/s]	Car Velocity (2) [m/s]
0.002	0.88	-0,88
0.024	-0,61	0.64

During this period, velocity changes occur rapidly. Consequently, if the sampling frequency falls below the required minimum, critical information can be lost, and the recorded signal may be distorted.

An adequate sampling frequency is crucial to accurately reconstruct the signal from sampled data. The Nyquist-Shannon theorem, applicable to various signals, including polynomial signals, mandates that the sampling frequency must be at least twice the highest frequency present in the signal to ensure accurate reconstruction [13]. For polynomial signals, which are not inherently periodic and thus lack an intrinsic frequency, the highest frequency corresponds to the maximum rate of oscillation of the polynomial function. This frequency can be determined by the function's maximum rate of change.

The maximum rate of change ( $T_{CM}$ ) is determined by evaluating the velocity function during the collision interval using Equation (1).

$$T_{CM} = \frac{\Delta v}{\Delta t} = \frac{v_f - v_0}{t_f - t_0}$$

$$T_{CM}(v_1) = \frac{\Delta v_1}{\Delta t} = \frac{(-0.62 - 0.88)}{0.024 - 0.002} = -68.18 \quad (1)$$

$$T_{CM}(v_2) = \frac{\Delta v_2}{\Delta t} = \frac{(0.62 - (-0.87))}{0.024 - 0.002} = 67.72$$

The velocity functions' rate of change, with values of -68.18 and 67.72, indicates a rapid variation. Although the absolute values of these rates are similar, the highest rate of change is 68.18. This value is critical for applying the Nyquist-Shannon theorem ( $F_{NyS}$ ), which dictates that the minimum sampling frequency should be twice the maximum rate of change to capture the signal accurately, (see equation (2)).

$$T_{cm}(v_1, v_2) = 68.18$$

$$F_{NyS} = 2 * T_{cm} = 136.36 \quad (2)$$

The minimum necessary sampling frequency is determined to be 136.36 Hz. However, to ensure optimal signal reconstruction, a sampling frequency exceeding this minimum requirement was utilized. Consequently, a sampling frequency ( $f_m$ ) of 500 Hz was established for this study.

Over 0.024 seconds and at the defined sampling frequency, twelve data points were recorded, referred to as the number of data points ( $N_d$ ), see equation (3).

$$\begin{aligned} N_d &= f_m * t \\ N_d &= 500 * 0.024 = 12 \end{aligned} \quad (3)$$

This number of data points is suitable for reconstructing the signals in question, given that the experimentation spans 0.024 seconds.

### 3. Results and Discussion

Within the framework of the analysis, multiple collisions were simulated. During these collisions, the test vehicles did not undergo permanent deformations or experience changes in mass. Velocities were continuously monitored, and data were systematically recorded within the designated time interval.

The multiple tests consistently demonstrated similar patterns and velocity values during the contact period, as illustrated in Figure 3.

As indicated in Figure 3, at the initial observation time, the vehicles exhibit average velocities of 0.88 m/s and -0.87 m/s, respectively. The opposite signs of these velocities indicate that the vehicles are moving in opposite directions. Over time, the velocities of both vehicles decrease.

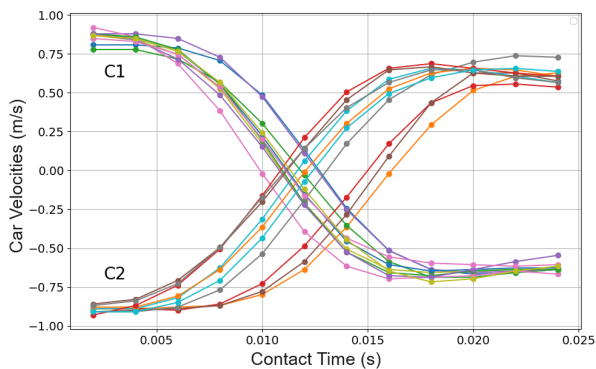


**Figure 3.** Car velocities during the contact time in the collision

This observation suggests that a braking force acts on the cars upon contact. At approximately 0.014 seconds, the velocities of both cars change signs, indicating a reversal in their directions of motion. From 0.014 seconds onward, the velocities of the vehicles continue to fluctuate, displaying different magnitudes

and directions; car 1 exhibits negative velocities, and car 2 exhibits positive velocities, showing that they are moving in directions opposite to their initial ones. By 0.024 seconds, it is evident that the velocities of both cars have diminished in magnitude, attributed to the presence of dissipative forces such as friction, which lead to energy loss.

A regression analysis was performed to determine the mathematical functions that most accurately fit the data. This analysis revealed that a fifth-degree polynomial function provides the most suitable model for the available data.

Experimentation in a controlled environment may be subject to inherent variations and errors, such as measurement inaccuracies or the physical conditions of the instruments used. Nonetheless, the replication of similar data across experiments indicates consistency in the findings. To mitigate the impact of these potential errors on the analysis, averaging the velocities during the contact period proves beneficial, as illustrated in Figure 4.

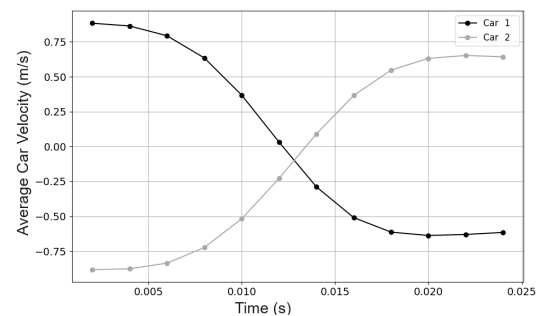


**Figure 4.** Average velocities of the cars during the contact time in the collision

#### 3.1. Kinematics of Car 1

Figure 5 illustrates the variation of velocity during the contact time in the collision. The behavior of this variation is best modeled by a fifth-degree polynomial function, expressed as:  $v(t) = -5E9t^5 + 3E8t^4 - 5E6t^3 + 28990t^2 - 66,985t + 0.9339$ .

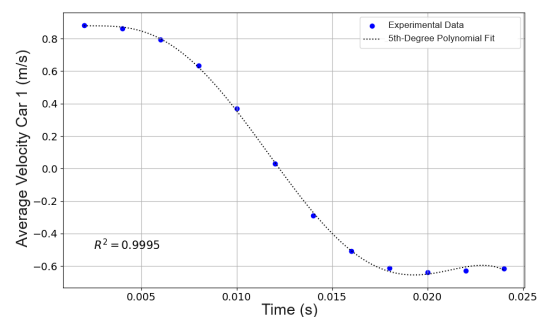


**Figure 5.** Variation of velocity as a function of time for Car 1 during the contact time in the collision

The curve fitting process yielded a coefficient of determination  $R^2 = 0,9995$ . A coefficient value close to 1 indicates a strong fit of the model to the data, meaning that 99.95% of the variability in the data is explained by the polynomial function.

At  $t = 0,002[s]$  seconds, the initial velocity of the car is  $0,88[m/s]$ . From  $t = 0,002[s]$  seconds to  $t = 0,012[s]$  seconds, the velocity decreases from  $0,88[m/s]$  to  $0,03[m/s]$ . From 0.012 seconds onward, the velocity changes from positive to negative, indicating a reversal in the direction of motion. Following this change, the velocity increases in magnitude, reaching  $-0,64[m/s]$  at  $t = 0,020[s]$  seconds. Beyond 0.020 seconds, the velocity tends to stabilize around  $-0,64[m/s]$ .

### 3.2. Kinematics of Car 2

The mathematical function that best describes the velocity variation of Car 2 is also a fifth-degree polynomial:  $v(t) = 4E9t^5 - 3E8t^4 + 6E6t^3 - 43570t^2 + 135,4t - 1,023$ , as illustrated in Figure 6.

The coefficient of determination  $R^2$  for this curve fitting is 0.9999, indicating an excellent fit of the model to the data. This value signifies that 99.99% of the variability in the dependent variable is explained by the polynomial function.

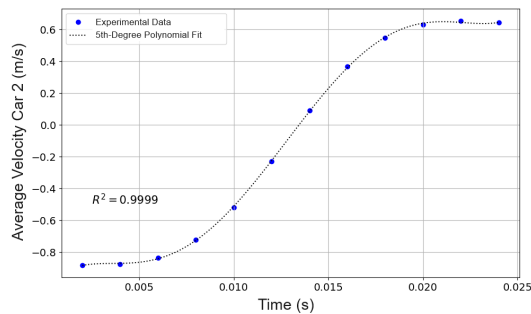


**Figure 6.** Variation of velocity as a function of time for Car 2 during the contact time in the collision

At  $t = 0,002$  seconds, the initial velocity of the car is  $-0.87$  m/s. The negative sign indicates that the vehicle is moving in the opposite direction to the chosen reference. The velocity decreases from  $-0.87$  m/s to  $-0.22$  m/s over the next 0.012 seconds. Subsequently, the velocity changes direction and begins to increase. At 0.014 seconds, the velocity is  $0.09$  m/s, indicating that the car has reversed direction. Following this change in direction, the velocity steadily increases, reaching  $0.63$  m/s at 0.024 seconds.

### 3.3. Coefficient of Restitution

For the analysis of the coefficient of restitution, Newton's kinematic impact law ( $\epsilon_n$ ) is applied as described by Equation (4), [14].

$$\epsilon_N = \frac{v^+}{u^-}, \quad 0 \leq \epsilon_N \leq 1 \quad (4)$$

Where the coefficient of restitution is the ratio of the relative velocities of the colliding bodies at the moments of contact and separation, as stated in the literature [15], ( see Figure 7).

Consequently, the magnitude of the average velocity at the end of contact ( $v_1 = 0,64$ ) for Car 2 decreased by 29.55% compared to the magnitude of the average velocity at the beginning of contact ( $u_1 = -0,88$ ).

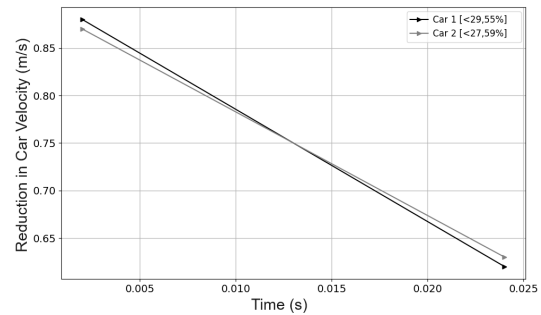


**Figure 7.** Variation in the magnitude of velocities during the contact time in the collision

The magnitude of the average velocity for Car 1 at the end of contact ( $v_2 = -0,61$ ) decreased by 27.59% compared to the magnitude of the average velocity at the beginning of contact ( $u_2 = 0,88$ ). Under these conditions, the coefficient of restitution calculated using Equation (4) is  $\epsilon_N = 0,712$ .

A coefficient of restitution between 0 and 1 indicates that the collision is partially elastic. This means that some of the kinetic energy is lost during the collision, manifesting as heat, sound, deformation, or other forms of non-kinetic energy.

### 3.4. Impulsive Forces

The variation in velocities during an impulse occurs over a very short interval ( $\Delta t$ ), associated with a high-value impulsive force [16]. Impulse theory hypothesizes that the duration of the impulse interval is brief, allowing the phenomenon to be considered practically instantaneous. In physics, the impulse is defined as the change in the momentum of an object and is related to the force ( $F$ ) and the differential time ( $dt$ ) during which that force acts [16]. Refer to Equation (5).

$$I = \int_{t_1}^{t_2} F dt \quad (5)$$

Impulsive forces are responsible for changing the velocities of the cars during the collision. The experimentation enables the calculation of impulsive forces during contact time using Newton's second law without

assuming that the phenomenon is instantaneous. Figure 8 illustrates the impulsive forces acting at the moment of contact, which occurs at 0.022 seconds. These physical phenomena can be modeled using polynomial functions that accurately describe the system's behavior and predict its evolution during the contact time.

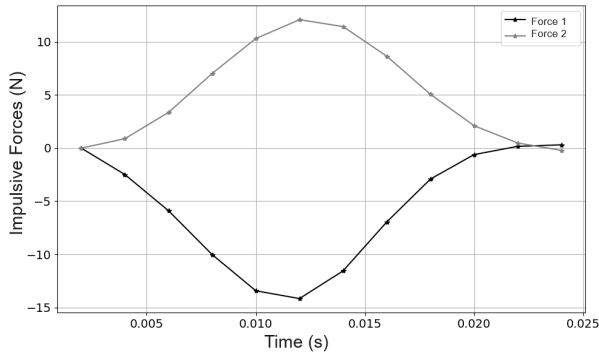


**Figure 8.** Impulsive forces during the contact time in the collision

The impulsive forces acting on Cars 1 and 2 exhibit different behaviors over time. Force 1 and 2 are oppositely directed, with the magnitude of Force 1 varying more significantly compared to Force 2.

The curve fitting for the impulsive forces of Cars 1 and 2 was performed using the coefficient of determination  $R^2$  as the criterion, with a value close to 1 indicating a better fit.

The curve fitting for Impulsive Force 1 (Figure 9) and Impulsive Force 2 (Figure 10) was achieved using a fifth-degree polynomial function:

$$\begin{aligned}
 F_1(t) &= 9E10x^5 - 7E9x^4 + 2e8x^3 \\
 &\quad - 2e6x^2 + 7179,7x - 7,8949 \\
 R^2 &= 0,9901 \\
 F_2(t) &= -3e11x^5 + 3e10x^4 - 1e8x^3 \\
 &\quad + 1e6x^2 + 5414,2x + 6,4383 \\
 R^2 &= 0,9944
 \end{aligned}
 \tag{6}$$

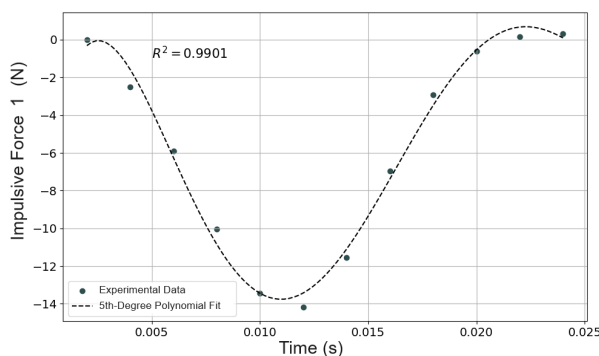


**Figure 9.** Curve fitting of impulsive force 1 during the contact time in the collision

Figure 9 illustrates that the impact force of Car 1 reached its maximum value  $F_{I1} = -14,171[N]$  in a relatively short time  $t_{I1} = 0,012[s]$ , indicating a rapid transfer of energy between the colliding objects.

Figure 10 illustrates that the impact force of Car 2 reached its maximum value  $F_{I2} = 12,097[N]$  in a relatively short time  $t_{I2} = 0,012[s]$ .

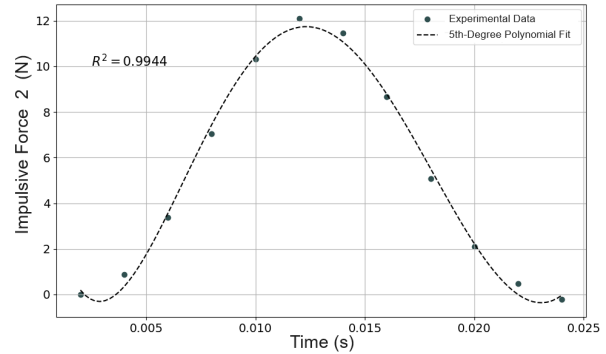


**Figure 10.** Curve fitting of impulsive force 2 during the contact time in the collision

The average time at which the impulsive forces reach their maximum value is 0.012 seconds. In a real impact scenario, this duration is critical, as the maximum magnitude of the force occurs within this interval. Therefore, establishing an airbag reaction time of less than 0.012 seconds in a real-world context becomes a crucial safety aspect. Implementing such a rapid reaction time in airbag systems would help mitigate the effects of impact forces, thereby reducing the risk of injury to vehicle occupants.

## 4. Conclusions

Understanding the variations in velocity, impulsive forces, and contact time during a collision is crucial for optimizing restraint systems such as seatbelts and airbags. This optimization ensures that these systems provide maximum protection at the critical moment of impact. As stated by Guazhambo and Larrea in their thesis from Universidad Politécnica Salesiana, titled "Database of Airbag Functionality in Vehicles Undergoing RTV in Cuenca, Determining Compliance with RTE INEN 034," this optimization is vital to enhancing vehicle safety.

Theoretical models may suggest perfectly elastic collisions with a restitution coefficient of 1. However, in practice, various real-world factors affect collisions, contributing to imperceptible deformations, friction, and energy loss. These factors make achieving a restitution coefficient of 1 in laboratory experiments challenging, if not impossible. Pursuing more realistic models and a deeper understanding of the sources of energy loss is essential for interpreting and applying experimental results effectively.

This research has modeled velocity-time and force-time functions as fifth-degree polynomial functions, capturing the variation of velocities and forces over 25 milliseconds. These models indicate nonlinear behavior with accelerated growth and decay. Understanding the kinematics of collisions at this scale, including relative velocity, impact force, and contact duration, can help detect the occurrence of a collision, determine when the peak value of impulsive forces is reached, and identify the optimal timing for activating passive safety systems.

Analyzing and understanding dynamic interaction processes can lead to exploring concepts in nanotechnology, where physical and chemical processes occur on infinitesimal scales. Therefore, future work should consider using mathematical models for simulating and analyzing physical processes at the nanoscale. This approach could help anticipate the behavior of velocity and force over extended periods and allow for comparisons with experimental data. Additionally, it would be valuable to explore which variables are represented by each of the coefficients in the velocity and force functions.

In the educational field, the experimental kinematics analysis in elastic collisions between two bodies during contact time allows students to apply theoretical concepts practically. This hands-on approach enhances their understanding and appreciation of Physics.

## References

- [1] C. E. Donoso-León, M. M. Paredes-Godoy, M. M. Gallardo-Donoso, and A. F. Samaniego-Campoverde, “El laboratorio virtual en el aprendizaje procedimental de la asignatura de física,” *Polo del Conocimiento*, vol. 6, no. 6, pp. 167–181, 2021. [Online]. Available: <https://doi.org/10.23857/pc.v6i6.2748>
- [2] P. M. Parra, *Uso de los Smartphones en los laboratorios de prácticas de física*. Universidad de Valladolid. España, 2017. [Online]. Available: <https://rb.gy/34xzk0>
- [3] P. Morcelle del Valle, *Transductores - instrumentación*. Universidad Nacional de la Plata, 2018. [Online]. Available: <https://rb.gy/iz42rz>
- [4] J. A. Osorio Cortéz, H. B. Cano Garzón, and J. A. Chaves Osorio, “Fundamentos y aplicación del muestreo en señales ubicadas en las bandas altas del espectro,” *Scientia Et Technica*, 2008. [Online]. Available: <http://rb.gy/ctv6el>
- [5] B. I. Guazhambo Loja and D. J. Larrea Vásconez, *Base de datos del funcionamiento del airbag en los vehículos que realizan la RTV en la ciudad de Cuenca, determinando el cumplimiento de la RTE INEN 034*. Universidad Politécnica Salesiana, 2022. [Online]. Available: <http://rb.gy/qnnc4f>
- [6] A. González Mateo, *Sensores en los sistemas de seguridad del automóvil*. Universidad de Valladolid, 2019. [Online]. Available: <http://rb.gy/du99uh>
- [7] D. A. Jerez Mayorga, L. X. Orbea Hinojosa, E. P. Gualotuña Quishpe, J. A. Toapaxi Csanoba, and J. A. y Rodríguez Rodríguez, “Diseño de un protocolo de pruebas del sistema airbag mediante la interpretación de oscilogramas de operación,” *INNOVA*, vol. 2, no. 9, pp. 135–146, 2017. [Online]. Available: <https://doi.org/10.33890/innova.v2.n9.2017.482>
- [8] E. I. Ayala Yunga and L. E. Tacuri Tacuri, *Análisis de la implementación de un sistema de airbag en autobuses en la seguridad del conductor durante un impacto frontal*. Universidad Politécnica Salesiana, 2021. [Online]. Available: <http://rb.gy/ui4ppl>
- [9] A. Cantero Díaz, M. M. Goire Castilla, and Y. Quintana Cassulo, “Sistema para la gestión y análisis de datos de una red de sensores inalámbricos basado en un almacén de datos.” *Revista Cubana de Ciencias Informáticas*, 2019. [Online]. Available: <https://is.gd/C094kY>
- [10] R. Hibbeler, *Dinámica. Mecánica Vectorial Para Ingenieros*. Pearson Education, 2004. [Online]. Available: <https://n9.cl/o1itx>
- [11] J. González-Laprea and A. Santiago, “Sistema automatizado para medición del coeficiente de fricción estática. un dispositivo para actividades de docencia,” *Revista Brasileira de Ensino de Física*, vol. 43, p. e20210056, 2021. [Online]. Available: <https://doi.org/10.1590/1806-9126-RBEF-2021-0056>
- [12] R. A. Serway and J. W. Jewett, *FÍSICA para ciencias e ingeniería*. CENGAGE Learning, 2005. [Online]. Available: <https://is.gd/LGiUOW>
- [13] M. Semeria, *Los tres teoremas: Fourier - Nyquist - Shannon*. ECONSTOR, 2015. [Online]. Available: <https://is.gd/t8NENe>
- [14] O. A. Rivera Ocampo, *Prototipo para el análisis dinámico del sistema leva-péndulo con impactos*. Universidad Nacional de Colombia, 2015. [Online]. Available: <https://is.gd/5aOwIx>
- [15] O. D. Pavioni and F. M. Ortega, “Obteniendo los coeficientes de restitución y arrastre en un solo experimento,” *Revista Mexicana de Física E*, 2015.

[16] J. M. Goicolea Ruigómez, *Curso de mecánica, vol. I y II*. Universidad Politécnica de Madrid, 2010.

[Online]. Available: <https://is.gd/fzo4OI>